

# Analysis of lncRNA-miRNA-mRNA Expression in the Troxerutin-Mediated Prevention of Radiation-Induced Lung Injury in Mice

Nan Zhang<sup>1,\*</sup>, Gui-yuan Song<sup>2,3,\*</sup>, Yong-jian Hu<sup>4</sup>, Xia Wang<sup>4</sup>, Tian-zhu Chao<sup>1</sup>, Yao-yao Wu<sup>1</sup>, Ping Xu<sup>1</sup>

<sup>1</sup>School of Food and Biomedicine, Zaozhuang University, Zaozhuang, Shandong, 277160, People's Republic of China; <sup>2</sup>School of Public Health, Weifang Medical University, Weifang, Shandong, 261000, People's Republic of China; <sup>3</sup>Radiology Laboratory, Central Laboratory, Rizhao People's Hospital, Rizhao, Shandong, 276800, People's Republic of China; <sup>4</sup>Henan Key Laboratory of Medical Tissue Regeneration, Xinxiang Medical University, Xinxiang, Henan, 453003, People's Republic of China

\*These authors contributed equally to this work

Correspondence: Ping Xu, Tel +86 19863349848, Email 13273730271@163.com

**Background:** Radiation-induced lung injury (RILI) is a critical factor that leads to pulmonary fibrosis and other diseases. lncRNAs and miRNAs contribute to normal tissue damage caused by ionizing radiation. Troxerutin offers protection against radiation; however, its underlying mechanism remains largely undetermined.

**Methods:** We established a model of RILI in mice pretreated with troxerutin. The lung tissue was extracted for RNA sequencing, and an RNA library was constructed. Next, we estimated the target miRNAs of differentially expressed (DE) lncRNAs, and the target mRNAs of DE miRNAs. Then, functional annotations of these target mRNAs were performed using GO and KEGG.

**Results:** Compared to the control group, 150 lncRNA, 43 miRNA, and 184 mRNA were significantly up-regulated, whereas, 189 lncRNA, 15 miRNA, and 146 mRNA were markedly down-regulated following troxerutin pretreatment. Our results revealed that the Wnt, cAMP, and tumor-related signaling pathways played an essential role in RILI prevention via troxerutin using lncRNA-miRNA-mRNA network.

**Conclusion:** These evidences revealed that the abnormal regulation of RNA potentially leads to pulmonary fibrosis. Therefore, targeting lncRNA and miRNA, along with a closer examination of competitive endogenous RNA (ceRNA) networks are of great significance to the identification of troxerutin targets that can protect against RILI.

**Keywords:** troxerutin, radiation-induced lung injury, ceRNA, lncRNA-miRNA-mRNA network, AKT, wnt signal pathway

## Introduction

Radiation therapy is critical for tumor treatment; however, radiotherapy-induced damage of normal tissue often limits its use and dosage. The lung is a highly sensitive organ to ionizing radiation. Studies revealed that about 10–20% of patients receiving chest radiotherapy exhibit radiation-induced lung injury (RILI), which can lead to other diseases, such as pulmonary fibrosis.<sup>1–3</sup> Therefore, reducing radiation-induced normal tissue damage is very important to the regulation of tumor treatment and enhancement of patient quality of life.<sup>4,5</sup> The continued development of new therapeutic methods or strategies requires an extensive comprehension of the basic molecular mechanism involved in RILI.

Non-coding RNA is identified as RNA that is transcribed, but does not encode protein. Micro-RNAs (miRNAs) are a form of endogenous single-stranded non-coding small-molecule RNAs ranging in 22nt. A modulatory feedback loop exists between lncRNA and miRNA.<sup>6–8</sup> lncRNA associates with miRNA as a competitive endogenous RNA (ceRNA), and participates in target gene expression modulation.<sup>9–11</sup> On the contrary, miRNA regulates lncRNA activity via the RNA-induced silencing complex (RISC). Both of these molecules are associated with multiple disease etiologies.<sup>12</sup>

RILI is a widespread complication of radiotherapy. However, its pathogenesis is unclear at the present time, and there is a lack of effective predictive indicators and treatment methods.<sup>13</sup> Current studies suggested that the lncRNA-miRNA-mRNA network

serves an essential function in radiation-mediated lung injury.<sup>14</sup> According to their reports, the T helpers (CD4<sup>+</sup> T cells) are critical in RILI, and their actions are mediated by the lncRNA-miRNA-mRNA network, thus accelerating fibrosis. This suggests that RNA disruption in the early stages of RILI produces severe late complications. Troxerutin is a flavonoid with anti-radiation and antioxidant properties, and it has aroused substantial research interest owing to its extensive pharmacological activities. Our previous research found that troxerutin enhanced radioprotection at least partially by activating AKT to inhibit the activation of JNK. Furthermore, troxerutin could increase the 30-day survival rates of irradiated mice and pre-administration with the effective dose of troxerutin reduced the hepatic damage induced by radiation.<sup>15-17</sup> At present, the radioprotective activity of troxerutin has been verified; however, its underlying mechanism remains to be elucidated.

Murine lungs are rich in lncRNAs, mRNAs, and miRNAs. However, there are limited studies on the role of lncRNA-miRNA-mRNA network in the troxerutin-mediated protection against RILI. Thus, this study employed RNA sequencing technology to clarify the lncRNA-miRNA-mRNA network-based mechanism of troxerutin action against RILI and to provide some ideas for RILI treatment.

## Materials and Methods

### Mouse Model of RILI

The 4-week-old RILI male C57BL/6- mouse model was acquired from the Beijing Unilever Co., Ltd. Three mice were housed in a single cage in standard laboratory environment (22 °C, 55% humidity, 12 h light/12 h dark cycle). Overall, six mice were separated into two groups: Troxerutin (0 mg/kg) and Troxerutin (10 mg/kg) were provided via intragastric administration for 4 days, respectively. Subsequently, all mice were irradiated with a single dose of 6 Gy X-ray exposure by using a linear accelerator (VitalBeam) at room temperature (23 °C±2 °C). The dose rate was 100 cGy/min. Radiation was obtained from the Department of Radiology of Rizhao people's Hospital. After irradiating once, all mice were sacrificed after 3 days, and the lung tissue was harvested. All experimental procedures and programs were conducted in accordance with the guidelines of the Care and Use of Laboratory Animals and approved by Science and Technology Ethics Committee of Zaozhuang University.

### Cell Culture and Cell Irradiation

The MTEC1, V79, and L-02 cells were purchased separately from the Shanghai Hongshun Biotechnology Co., Ltd., Beijing Dingguo Changsheng and Beina Chuanglian Biotechnology Co., Ltd. All cells were maintained in Roswell Park Memorial Institute (RPMI-1640) supplemented with 10% fetal bovine serum (FBS), 100 units/mL penicillin, and 100 mg/mL streptomycin. All cells were incubated at 37 °C in a humidified atmosphere containing 5% CO<sub>2</sub>. For drug treatment group, cells were treated with 10 µg/mL of troxerutin before irradiation. Cells were irradiated in a 6-well plate at the same dose as mice.

### Construction and Sequencing of the RNA Library

Total RNA from lung samples was isolated and purified using TRIzol (Invitrogen, Carls-bad, California). In the construction of lncRNA library, the quality of RNA was checked on Caliper Labchip GX using DNA 1K Reagent Kit. About 500 ng of murine RNA was used in the reaction system. RNase H kit was used to remove rRNAs. Then, RNA was fragmented. After that, the pre-segmented RNA was reverse transcribed into the first strand of cDNA. The second strand cDNA was synthesized under the action of dUTP. Next, the double-stranded cDNA fragment is repaired at the end, and a single "A" nucleotide was connected to the 3' end of the flat-end fragment. Then adapters were ligated to the cDNA. The cDNA was amplified by PCR. The reaction conditions were as follows: 3 minutes, 95°C for initial denaturation; 30 seconds, 95°C for 14 cycles of denaturation; 30 seconds, 56°C for annealing; 1 minute, 72°C for extension; 5 minutes, 72°C for final extension. In the construction of miRNA library, the quality of RNA was checked on Agilent 2100 Bioanalyzer using Agilent DNA 1000 Kit. After that, the 5000 ng RNA samples were taken and the 18–30nt RNA was recovered and purified by polyacrylamide gel electrophoresis. The purified RNA was connected to the 3' ends and 5' ends, and the reverse transcription and PCR amplification were carried out. The purpose bands of PCR were recovered by polyacrylamide gel electrophoresis and stored in EB buffer. The PCR products of the above two libraries were denatured into single strands, and then cyclized to obtain single-stranded circular DNA molecules. The single-stranded circular DNA molecules were then replicated via rolling cycle amplification, and a DNA nanoball (DNB) containing multiple copies of

DNA was generated. Sufficient quality DNBS were then loaded into patterned nanoarrays using high-intensity DNA nanochip technique, and sequenced using combinatorial Probe-Anchor Synthesis (cPAS).

## The lncRNA-miRNA-mRNA Network Generation, Expression, and Functional Analyses

To start, sequencing data filtration was done via SOAPnuke, clean reads were retrieved, then stored in the FASTQ format. Subsequent analysis and data mining were performed on Dr Tom Multi-omics Data mining system (<https://biosys.bgi.com>). Following filtration, the clean tags were mapped to the reference genome and other sRNA database using Bowtie2. Subsequently, RNAhybrid, miRanda, and TargetScan were employed for lncRNA and miRNAs target gene estimation, and to visualize the lncRNA-miRNA-mRNA networks. Relative gene expression was determined by RSEM (v1.3.1). In particular, differentially expressed (DE) gene analysis was conducted via DESeq2 (v1.4.5) with Q value  $\leq 0.05$ . To conduct functional analysis, both GO and KEGG enrichment analyses of annotated DE genes were carried out via Phyper based on the Hypergeometric evaluation. Significant terms and networks were corrected by the Q value using a strong cut-off value (Q value  $\leq 0.05$ ).

## Results

### H&E Staining of Radiation Induced Lung Injury

In order to determine whether the RILI model has been successfully prepared and verify the protective effect of troxerutin, we compared the lung tissue of irradiated mice, irradiated mice pretreated with troxerutin and the control group by H&E staining. According to our HE results, the lung tissue of non-irradiated mice showed clear alveolar contour, closely arranged alveolar epithelial cells and complete histological morphology (Figure 1A). After 3 days of radiation, the integrity of the lung tissue of the irradiated mice without the intervention of troxerutin was seriously damaged, the alveolar interstitium of the mice was significantly increased, the alveolar volume was significantly reduced due to extrusion, and a large number of inflammatory cells infiltrated in the alveoli (Figure 1B). Nevertheless, troxerutin could reduce radiation damage, maintain the normal morphology of mouse lung tissue, and improve the pathological changes of mouse lung (Figure 1C).

### The Relative mRNA, lncRNA, and miRNA Expressions

Overall, 22064 mRNAs, 24239 lncRNAs, and 2959 miRNAs were detected in 6 mice. To better understand the differential gene expression in radiation-damaged mice pretreated with Troxerutin (TRT), we compared the expression profiles of lncRNA, mRNA, and miRNA between IR+TRT group (10 mg/kg) and IR group (0 mg/kg). Relative to the IR group mice, 184 mRNAs were markedly up-regulated and 146 mRNAs were considerably down-regulated. Similarly, 150 lncRNAs were markedly elevated, and 189 showed considerable downregulation. In terms of miRNA, 43 showed significant upregulation and 15 marked downregulation ( $Q < 0.05$ ,  $|\log_2FC| > 1$ ). The most up-regulated lncRNA was Tbrg3 (21378), and the most down-regulated lncRNA was Gm9901 (102640773). The most up-regulated miRNA was

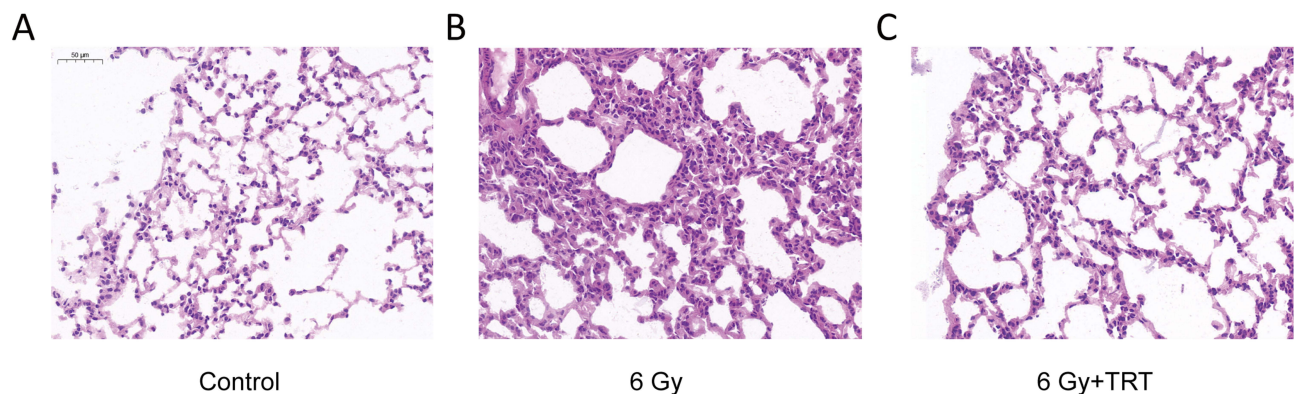


**Figure 1** H&E staining of lung tissue at 72 h after radiation. Compared with the control group (A), the radiation-induced lung injury (6 Gy) group (B) showed thickened alveolar walls, alveolar septal edema, and massive inflammatory cell infiltration in the alveoli. The troxerutin pretreatment group (6 Gy+TRT) (C) could reduced the damage caused by radiation, maintained the normal morphology of lung tissue in mice.

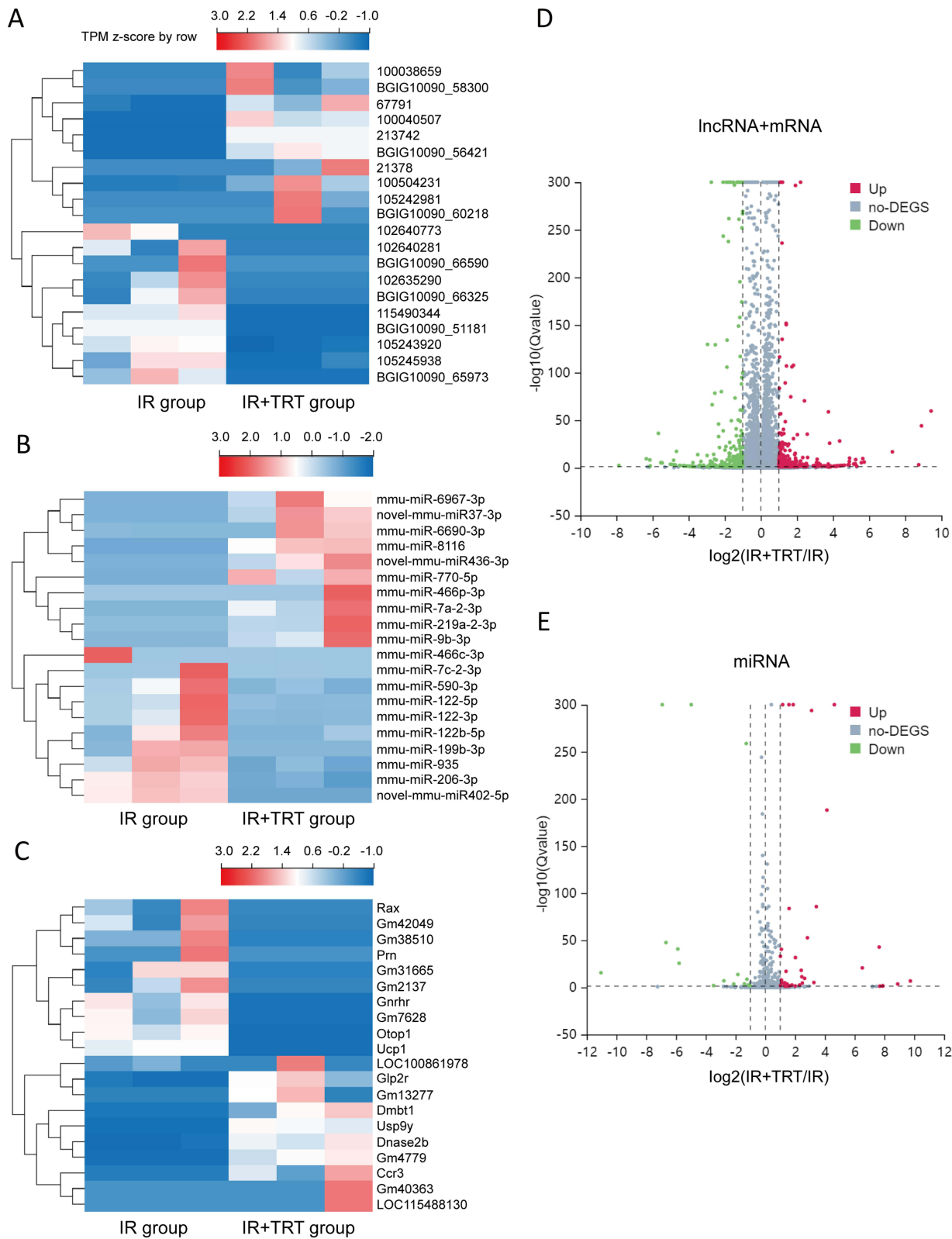


**Figure 2** The expression profiles of lncRNAs, miRNAs, and mRNAs in the radiation-induced lung injury (RILI) and Troxerutin pre-treated mice. A total of 150 upregulated and 189 downregulated lncRNAs are displayed in **(A)** the heat map and **(D)** the volcano plot; 43 upregulated and 15 downregulated miRNAs are displayed in **(B)** the heat map and **(E)** the volcano plot; and 184 upregulated and 146 downregulated mRNAs are displayed in **(C)** the heat map and **(D)** the volcano plot. Red represents upregulation and blue represents downregulation.

novel-mmu-miR436-3p, which enhanced 9.74 times, and the most down-regulated miRNA was novel-mmu-miR402-5p, which reduced by 11.04 times. The most up-regulated mRNA was Usp9y, which increased by 9.43 folds, and the most down-regulated mRNA was Ucp1, which decreased by 5.67 folds (Figure 2A–C). The differential lncRNA, mRNA, and miRNA expressions between the two groups are presented as volcanic maps (Figure 2D and E). In addition, the top 5 lncRNA, mRNA, and miRNA up-regulations and down-regulations are summarized in Tables 1–3.

**Table 1** Top 5 Significantly Up- and Downregulated Long Noncoding RNAs

Gene ID	Gene Symbol	log <sub>2</sub> (6 Gy_TRT/6 Gy)	Q value
21378	Tbrg3	8.90	<0.05
BGIG10090_58300	BGIG10090_58300	8.75	<0.05
105242981	Gm39041	7.29	<0.05
BGIG10090_60218	BGIG10090_60218	5.73	<0.05
100504231	Gm15708	5.65	<0.05
115490344	LOC115490344	-5.54	<0.05
BGIG10090_51181	BGIG10090_51181	-6.13	<0.05
BGIG10090_66590	BGIG10090_66590	-6.15	<0.05
BGIG10090_65973	BGIG10090_65973	-6.34	<0.05
102640773	Gm9901	-7.86	<0.05

**Table 2** Top 5 Significantly Up- and Downregulated MicroRNAs

Gene ID	log <sub>2</sub> (6 Gy_TRT/6 Gy)	Q value
novel-mmu-miR436-3p	9.74	<0.05
mmu-miR-7a-2-3p	8.89	<0.05
mmu-miR-219a-2-3p	7.89	<0.05
mmu-miR-8116	7.89	<0.05
novel-mmu-miR37-3p	7.88	<0.05
mmu-miR-122-3p	-5.79	<0.05
mmu-let-7c-2-3p	-5.88	<0.05
mmu-miR-466c-3p	-6.67	<0.05
mmu-miR-199b-3p	-6.92	<0.05
Novel-mmu-miR402-5p	-11.04	<0.05

**Table 3** Top 5 Significantly Up- and Downregulated Messenger RNAs

Gene ID	Gene Symbol	log <sub>2</sub> (6 Gy_TRT/6 Gy)	Q value
107868	Usp9y	9.43	<0.05
56629	Dnase2b	5.26	<0.05
105244826	Gm40363	5.2	<0.05
115488130	LOC115488130	5.15	<0.05
100861978	LOC100861978	4.92	<0.05
105246825	Gm42049	-4.73	<0.05
21906	Otop1	-4.76	<0.05
111368	Prn	-4.81	<0.05
115487215	Gm7628	-5.46	<0.05
22227	Ucp1	-5.67	<0.05

## LncRNAs and miRNA Serve as CeRNAs via the lncRNA-miRNA-mRNA Network

To further examine the potential activities of maladjusted lncRNAs and miRNAs in radiation-induced injury in mice treated with troxerutin using the ceRNA networks, we selected all maladjusted lncRNAs and miRNAs to estimate their sequestration of miRNAs and target mRNAs, respectively. A Venn diagram was utilized to depict the association between the misaligned lncRNAs, the lncRNA-based sequestration of miRNAs, and the target mRNAs. As shown in Figure 3, we identified 23 sponge miRNA maladjustments of maladjusted lncRNAs, and 20 target mRNA maladjustments of maladjusted miRNAs. Next, we analyzed all the target mRNAs regulated by DE miRNA using GO. As depicted in Figure 4A, the transmembrane ephrin receptor activity, liver ligand receptor activity, as well as transmembrane receptor protein tyrosine and protein tyrosine kinase activities were the primary functions correlated with dysfunctional miRNAs.

We next analyzed the KEGG networks of the target mRNAs regulated by maladjusted miRNAs. The primary enrichment pathways and related genes included the Wnt-signaling pathway (Prickle1, Lgr4, Camk2d, Apc, Camk2b, Camk2g, Csnk2a1, Dvl1, Dvl2, Fzd5, Invs, Jun, Lrp6, Nfatc2, Prkacb, Ppp3r2, Rac2, Wnt8a, Tcf711, Wnt9b, Rspo2, Cxnc4, Gsk3b, Ctnnbip1, Daam2, Csnk1a1, Nkd1), cAMP signaling pathway (Camk2d, Adcy7, Adcyap1r1, Adora1, Adrb1, Akt2, Atp2a2, Atp2b2, Bad, Bdnf, Cacna1c, Cacna1s, Calm3, Camk2b, Camk2g, Chrm1, Gria1, Grin2a, Hcn2, Jun, Pik3ca, Pik3cd, Pik3r1, Prkacb, Rac2, Rock1, Cnga4, Pde4d, Abcc4, Grin3a, Adcy10) and pathways in cancer (Camk2d, Adcy7, Akt2, Apc, Xiap, Arnt, Bad, Bcl2l11, Calm3, Camk2b, Camk2g, Casp8, Cttna1, Runx1t1, Ccne2, Cdk6, Cxcr4, Col4a5, Cyes, Dvl1, Dvl2, E2f1, Ednr, Erbb2, Esr1, Fgf5, Fgfr3, Flt4, Fzd5, Gng4, Il15ra, Il5ra, Il7r, Jun, Kit, Lama1, Lrp6, Smad2, Mitf, Gadd45b, Nqo1, Nras, Pik3ca, Pik3cd, Pik3r1, Prkacb, Ptger4, Rac2, Rasgrp1, Rock1, Stat5a, Stat5b, Wnt8a, Tcf711, Vegfa, Wnt9b, Zbtb16, Sufu, Nco4, Lpar5, Gsk3b, Rps6ka5, Ccdc6, Lpar4) (Figure 4B). In addition, we also analyzed the KEGG axes of DE mRNAs and these three pathways were also enriched (Figure 4C).

## Troxerutin Inhibited JNK by Activation of AKT in Radioprotection

Analyses of KEGG pathways associated with the target genes of miRNAs differentially expressed in this study revealed the enrichment of Akt2 in tumor-associated signaling pathways, consistent with a model wherein troxerutin plays certain functional roles in protecting against radiation-induced pulmonary damage in line with our experimental findings pertaining to AKT1. To recapitulate the mouse experiments, the MTEC1, V79, and L-02 cells were separated into IR and IR+TRT groups, revealing the ability of troxerutin to activate AKT and to increase intracellular p-AKT and total AKT content in radioprotection (Figure 5). Upon AKT1 silencing, however, p-AKT and total AKT were largely undetectable in these cells. In contrast, AKT1 overexpression resulted in no detectable differences in the levels of p-AKT or total AKT when comparing the troxerutin group and the control group in radioprotection (Figure 6). For further

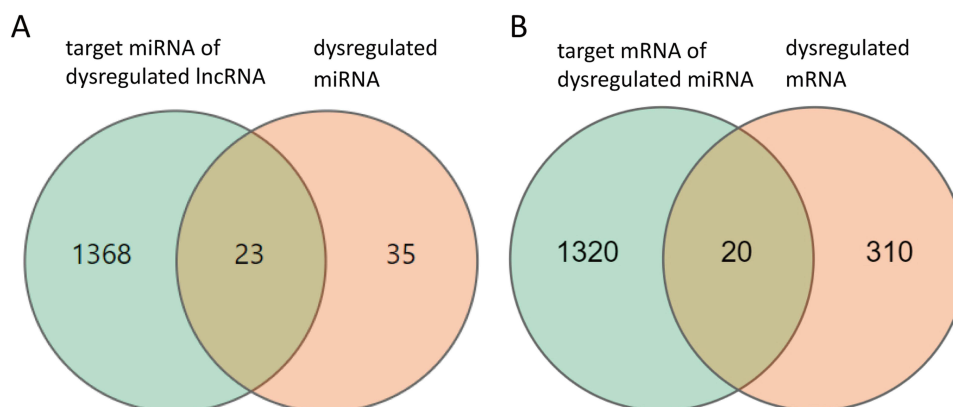


**Figure 3** Differentially expressed (DE) mRNAs, miRNAs, and lncRNAs, and their relationships. The red circle represents the 35 dysregulated miRNAs, the green circle represents the 1368 target mRNAs of dysregulated lncRNAs (A). The green circle represents the 1320 target mRNAs of dysregulated miRNAs, and the red circle represents the 310 dysregulated mRNAs (B).

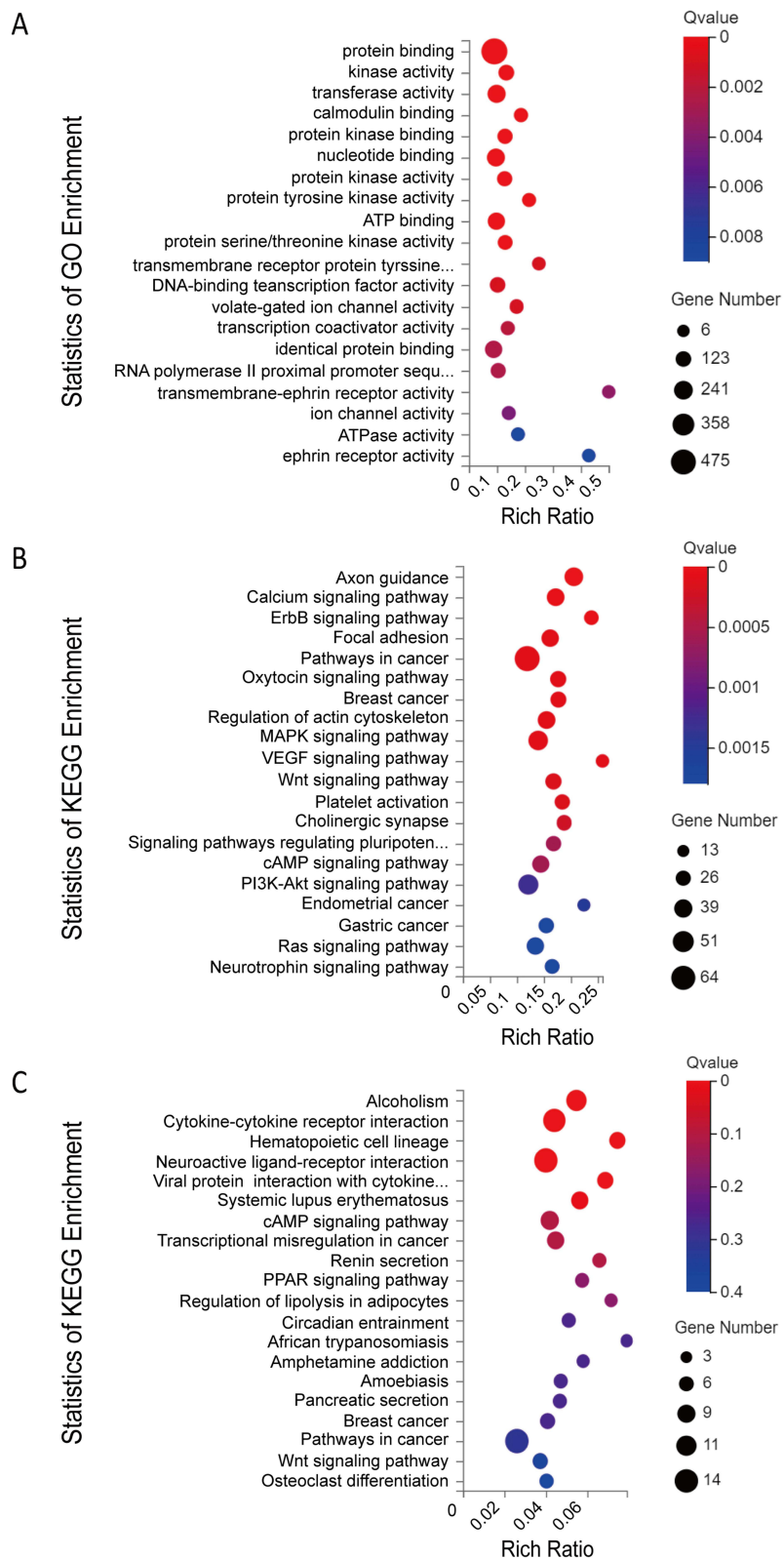


**Figure 4** (A) Gene Ontology (GO) annotations and (B) Kyoto Encyclopedia of Genes and Genomes (KEGG) pathway analysis of the mRNAs regulated by the lncRNA-miRNA-mRNA network; (C) KEGG pathway analysis of the dysregulated mRNAs. The top 20 according to Q value of each analysis are displayed.

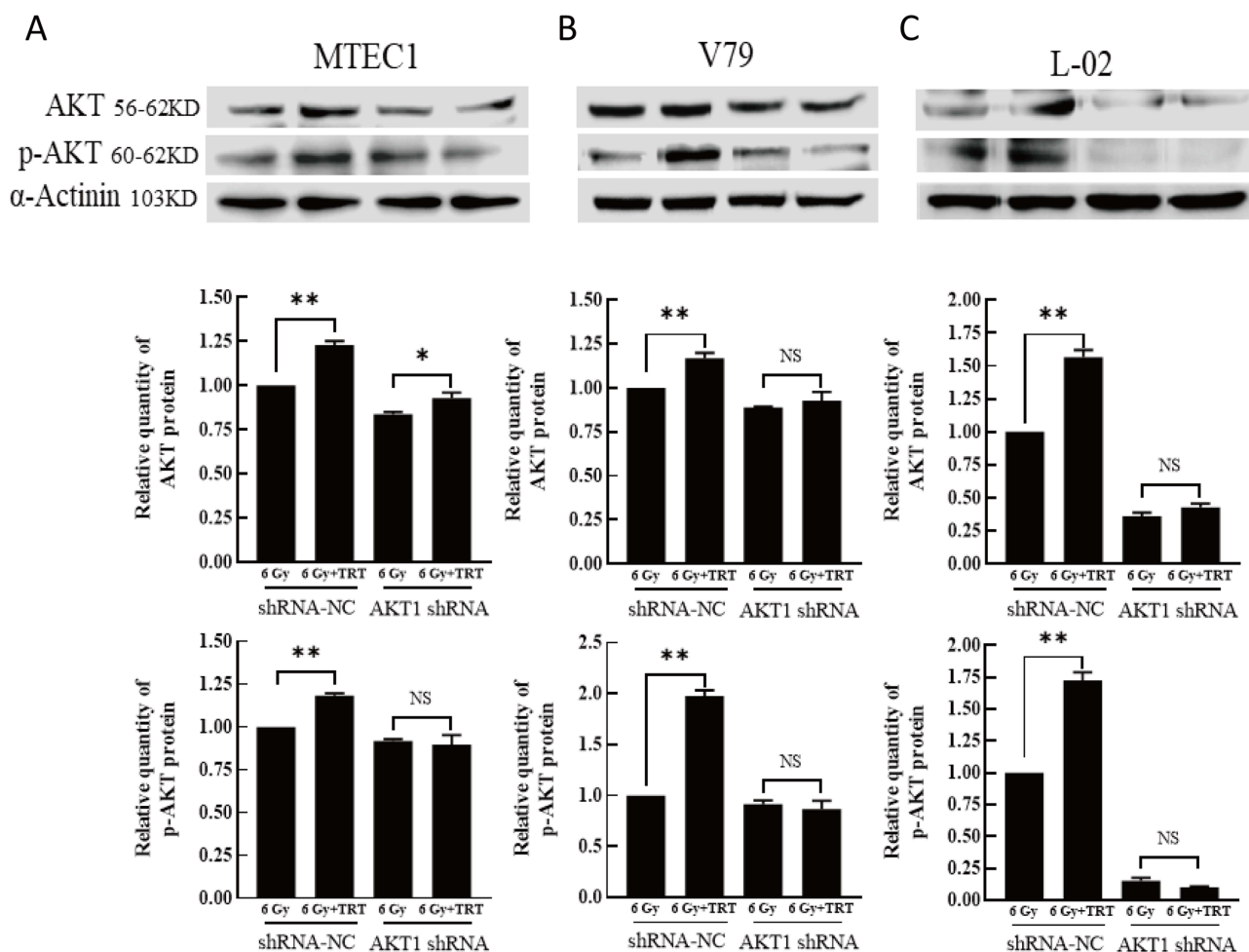


**Figure 5** The impact of AKT knockdown on the effects of TRT on p-AKT and total AKT levels. The p-AKT and AKT levels in MTEC1 (A), V79 (B), and L-02 (C) cells in the 6 Gy and 6 Gy+TRT groups were assessed by Western blotting, and results were analyzed by GraphPad Prism 8. \* $P < 0.05$ , \*\* $P < 0.01$ .

details regarding shRNA sequences, the results of sequencing analyses, and AKT overexpression plasmids, see [Supplementary Table S1-2](#) and [Supplementary Figures 1-2](#). To more fully elucidate the mechanisms through which AKT influences the pathogenesis of radiation-induced lung injury, the expression of the AKT downstream target protein JNK was analyzed. Pretreatment with troxerutin resulted in a significant increase in both p-JNK and total JNK levels in radioprotection ([Figure 7](#)). Knocking down AKT1 resulted in p-JNK activation at significantly higher levels than those observed following troxerutin pretreatment in radioprotection. Conversely, overexpressing AKT inhibited JNK phosphorylation, and p-JNK levels remained higher than in the troxerutin pretreatment group. Troxerutin is thus likely to protect lung cells against radiation-induced injury through the antagonism of radiation-mediated JNK activation.

## Construction of ceRNA Networks Based on the Identified mRNAs and Bioinformatics Estimation

To further elucidate the significance of these lncRNAs and miRNAs in Troxerutin-induced radiation injury prevention, we filtered the DE mRNAs from the transmembrane adrenoceptor active mRNAs using GO analysis, and constructed the lncRNA-miRNA-mRNA network. In total, we employed 100 lncRNA-miRNA-mRNA network, which included 33 lncRNAs, 50 miRNAs, and 17 mRNAs. Given the complex nature of the generated ceRNA axes, we constructed visual lncRNA-miRNA-mRNA network using the filtered RNAs ([Figure 8](#)), which may assist in the enhanced comprehension of such associations, and augment the comprehension of the mechanism underlying the troxerutin-mediated inhibition of

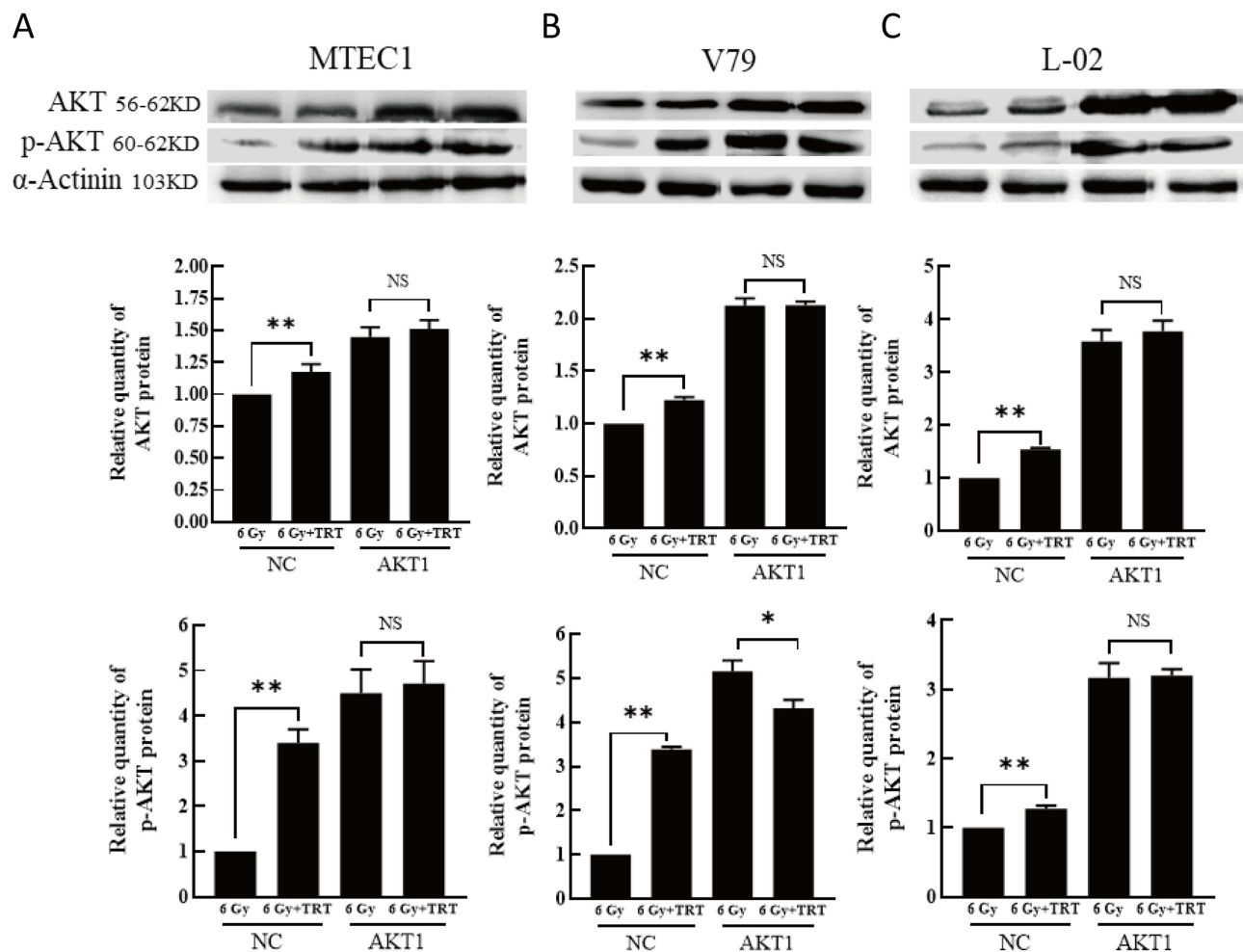


**Figure 6** The impact of AKT overexpression on the effects of TRT on p-AKT and total AKT levels. The p-AKT and AKT levels in MTEC1 (A), V79 (B), and L-02 (C) cells in the 6 Gy and 6 Gy+TRT groups were assessed by Western blotting, and results were analyzed by GraphPad Prism 8. \* $P < 0.05$ , \*\* $P < 0.01$ .

radiation injury. At the same time, Figure 9 is drawn to show the competition mechanism of the ceRNA network more intuitively.

## Discussion

RILI is a complicated process, which involves a myriad of molecular and cellular associations. Together, these interactions promote the broad-scale proliferation, differentiation, and accumulation of fibroblasts, which, in turn, results in the disproportionate deposition of extracellular matrix and pulmonary fibrosis. Troxerutin possesses anti-radiation protective property, however, the underlying mechanism remains undetermined. Hence, investigations are warranted to clearly identify targets and molecular mechanisms associated with the troxerutin-based prevention of RILI.

In some cases, the stability of lncRNA was reduced by the interaction of specific miRNAs. In other cases, lncRNAs can be used as bait for miRNAs, and the chelation of miRNAs was beneficial to the expression of target mRNAs that were inhibited. Other lncRNAs inhibit gene expression by competing with miRNAs and interacting with shared target mRNAs. Finally, some lncRNAs can produce miRNAs, resulting in inhibition of target mRNAs.<sup>18</sup> Therefore, integrated analysis of the regulatory relationship between lncRNA-miRNA-mRNA can more comprehensively explain the occurrence and development of diseases. However, the complex mechanism of lncRNA-miRNA-mRNA related to the prevention of radiation lung injury by troxerutin has not been fully understood. Herein, in our research, mice were pretreated with troxerutin prior to radiation, and both the control and troxerutin pretreated mice were irradiated

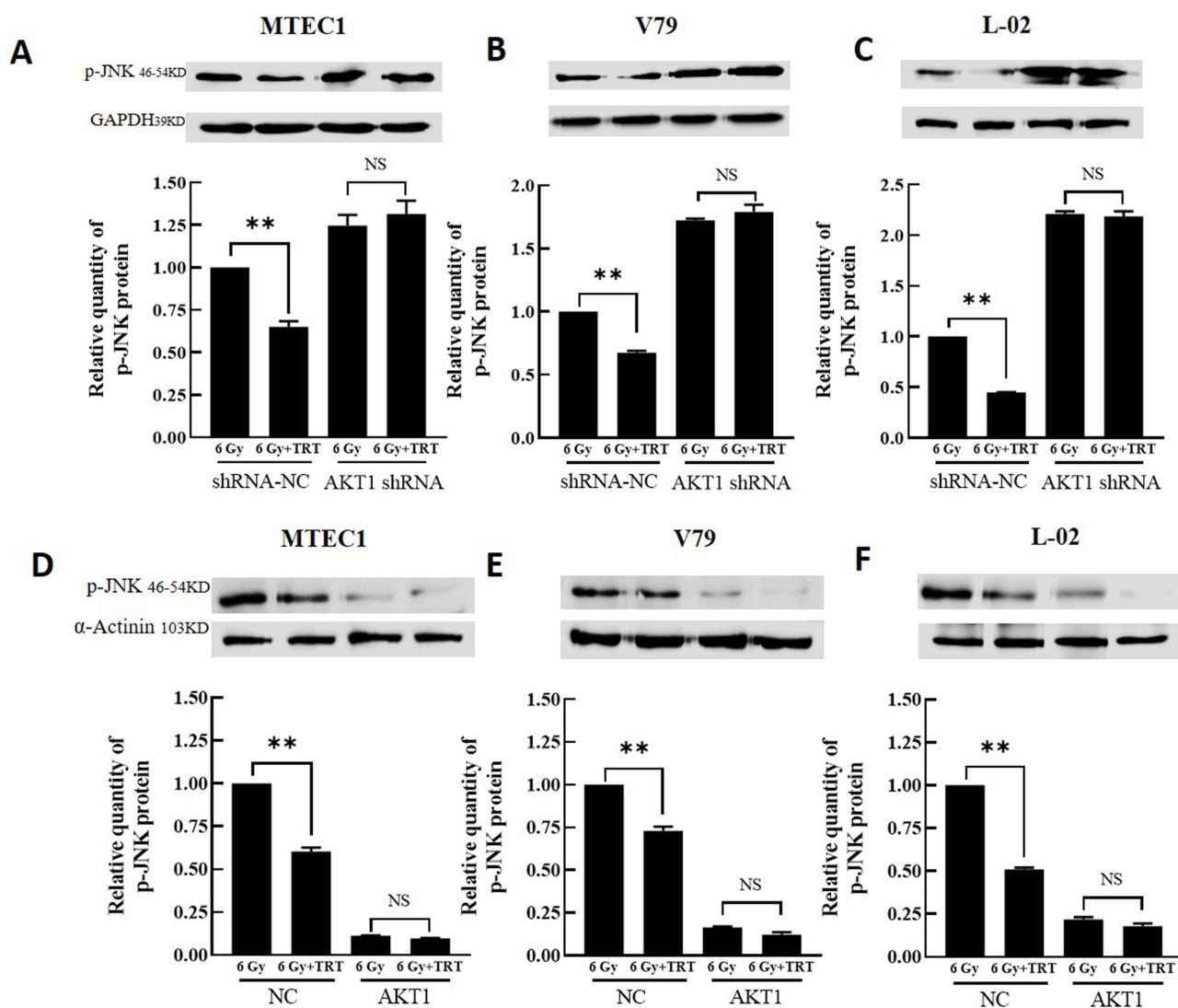


**Figure 7** The impact of overexpressing or silencing AKT on the expression of p-JNK and total JNK. The p-JNK and JNK levels in MTEC1 (A and D), V79 (B and E), and L-02 (C and F) cells in the 6 Gy and 6 Gy+TRT groups were assessed by Western immunoblotting, and results were analyzed by GraphPad Prism 8. \*\*P < 0.01.

simultaneously before assessment of the murine lung lncRNA, miRNA, and mRNA expressions using RNA sequencing. In total, we identified 727 DE genes, which included 377 highly expressed and 350 scarcely expressed genes.

Based on our KEGG analysis, the significantly maladjusted pathways included the cAMP, Wnt, and tumor-associated signaling pathways. The KEGG pathway analysis of all DE mRNAs also revealed the same results, suggesting that these signaling networks were modulated by troxerutin and radiation damage, and that it regulated both miRNA and downstream mRNA statuses. In the analysis of DE miRNA in gastric cancer, DE hsa-miR-148a-3p, hsa-miR-148b-3p, and hsa-miR-363-3p were markedly enriched in cancer-associated networks, namely, Wnt, which corroborated with our findings.<sup>19</sup> Other studies revealed that radiation activates the classical WNT/ $\beta$ -catenin signaling in HLF, and co-culture with HUMSCs weakens this activation in radiation-induced HLF, thereby inhibiting HLF myofibroblast differentiation. Wnt/ $\beta$ -Catenin axis is a potential therapeutic target against RILI in lung cancer patients who receive radiotherapy.<sup>20</sup> Our data revealed that troxerutin pretreatment-induced alterations in miRNAs and target mRNAs in the murine lung tissue. Moreover, it enriched the Wnt signaling pathway, which corresponded to a study that demonstrated that troxerutin stimulates the target gene expression downstream of the transcription factor  $\beta$ -catenin and Wnt signal, which confirms the activation of the Wnt/ $\beta$ -catenin signaling pathway.<sup>21</sup> Additionally, studies revealed that following troxerutin pretreatment, the miRNA expression changes, and the

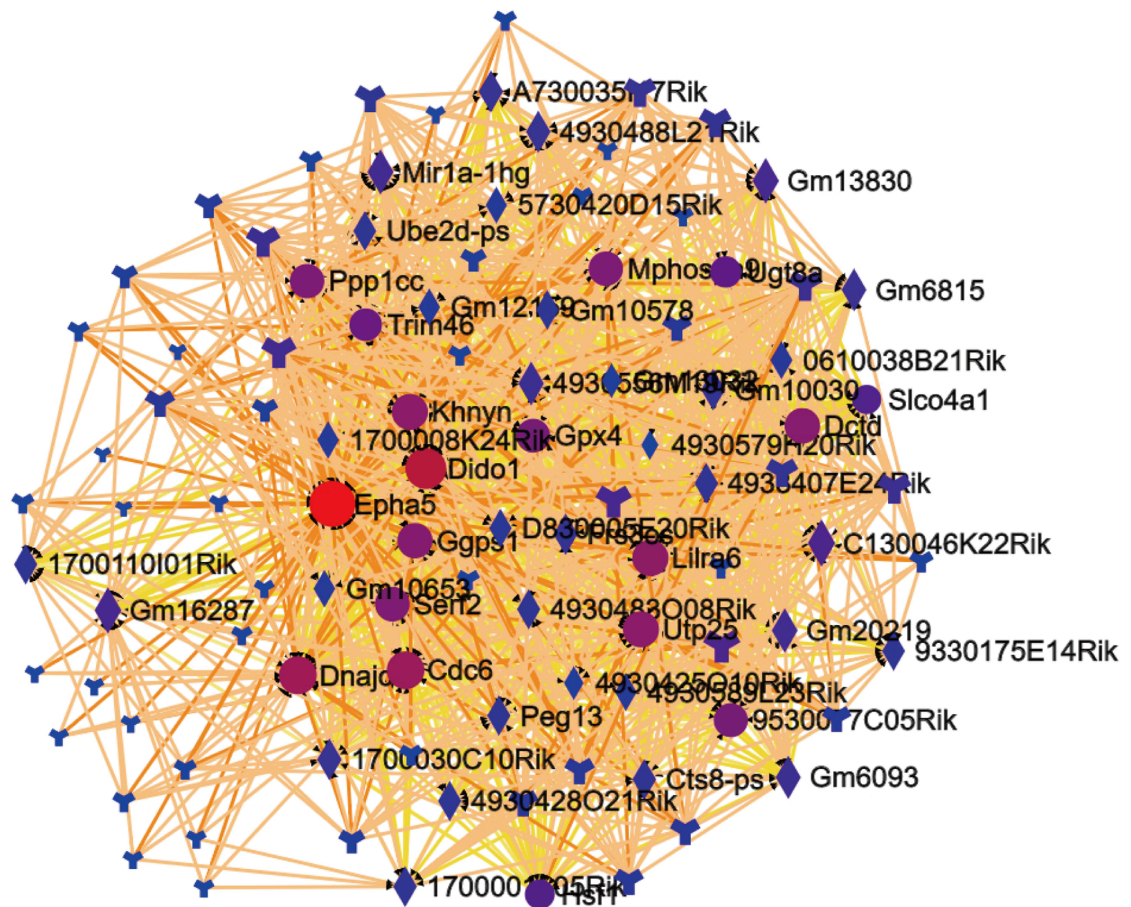
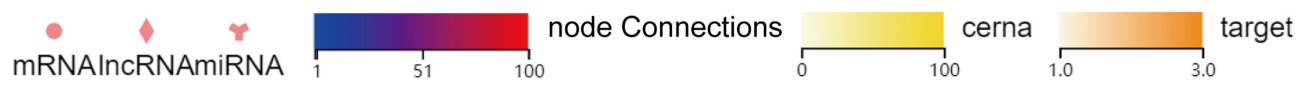


**Figure 8** The lncRNA-miRNA-mRNA network, based on the filtered mRNA associated with the transmembrane ephrin receptor activity in Gene ontology (GO) analysis. Dots represent mRNAs, square represents lncRNAs, and the branch shape represents miRNAs. Their regulatory relationships are displayed as lines between them.

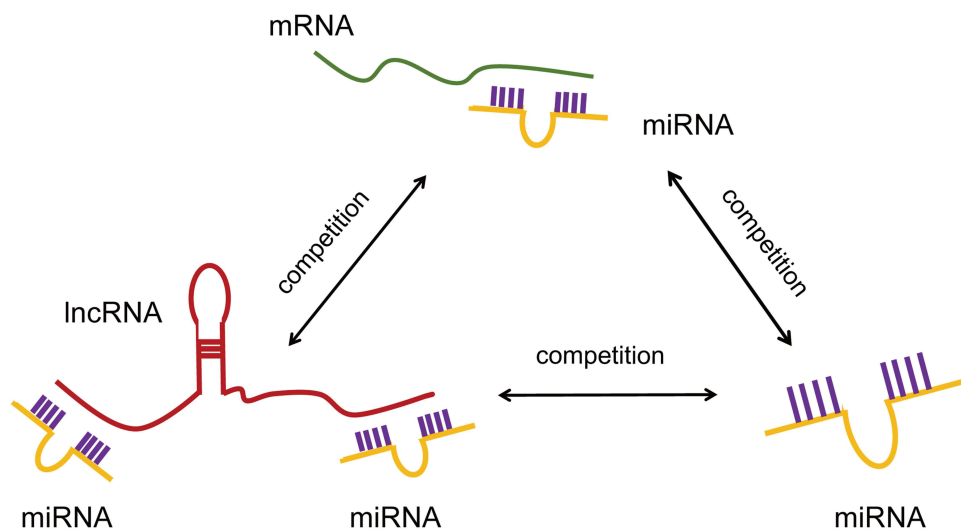


**Figure 9** The competition mechanism of the ceRNA network.

altered miRNA modulates several cellular signal pathways, including, mitogen-activated protein kinase and WNT pathways. The functional annotation of this study confirmed that the Wnt signaling pathway was regulated by the lncRNA-miRNA-mRNA network, which suggests that the pharmacological targeting of associated lncRNAs or miRNAs may potentially modulate the Wnt signaling pathway, thus providing a therapeutic target for troxerutin in preventing radiation injury.

In our study, through KEGG analysis of the target mRNA of differentially expressed miRNA, we found that AKT2 was enriched in tumor-related signaling pathways, which coincided with our cell experimental results, indicating that AKT-signaling pathway was involved in the expression of lncRNA-miRNA-mRNA network in TRT-regulated radiation-induced lung injury. Studies have shown that hypoxia and HIF-1  $\alpha$  could trigger ER stress and CHOP-mediated AECs apoptosis, suggesting that it may be involved in the development of idiopathic pulmonary fibrosis.<sup>22</sup> Hypoxia stimulates tumor cells to produce hypoxia-inducible factor-1  $\alpha$ , which induced the production of GLUT-1, which in turn increased glucose uptake and cell metabolism. PI3K/mTOR involved in cell metabolism was beneficial to aerobic glycolysis, which may prepare for the activation of AKT.<sup>23</sup> We speculate that these molecules may be involved in radiation lung injury as therapeutic targets, and troxerutin may be the first choice for targeted therapy.

In short, using RNA sequencing, we identified DE lncRNAs, miRNAs, and mRNAs, and we generated ceRNAs axes. Our KEGG analysis emphasized that the Wnt signaling pathway as well as AKT strongly modulates the troxerutin-based prevention of RILI using the lncRNA-miRNA-mRNA network. Therefore, further examination into the underlying mechanism and early intervention involving lncRNAs and miRNAs with associated ceRNA networks will be beneficial to RILI treatment.

## Conclusions

Our study revealed that the abnormal regulation of RNA potentially leads to pulmonary fibrosis and the Wnt, cAMP, and tumor-related signaling pathways played an essential role in RILI prevention via troxerutin using lncRNA-miRNA-mRNA network. Therefore, targeting lncRNA and miRNA, along with a closer examination of competitive endogenous RNA (ceRNA) networks are of great significance to the identification of troxerutin targets that can protect against RILI. However, our work failed to further verify more lncRNA-miRNA-mRNA network relationships, which will provide guidance for our future research.

## Abbreviations

RILI, Radiation-induced lung injury; IR, irradiation; TRT, Troxerutin; DE, differentially expressed; LncRNA, Lncoding RNA; miRNA, Micro-RNA; mRNA, messenger RNA; ceRNA, competitive endogenous RNA; KEGG, Kyoto Encyclopedia of Genes and Genomes; GO, Gene Ontology.

## Data Sharing Statement

The datasets used and/or analysed during the current study are available from the corresponding author on reasonable request.

## Ethics Approval and Consent to Participate

The protocol for animal experiment was approved by Science and Technology Ethics Committee of Zaozhuang University. Reference Number: ZZU-N007; Date: 2022-2-28.

## Acknowledgments

We thank Beijing Genomics institution (BGI) Gene Co., Ltd. for the sequencing work. Nan Zhang and Gui-yuan Song share first authorship.

## Funding

This work was supported by the National Science Foundation of China (NSFC) (Nos. 81773358, 11705158, U1504824), the Shandong Students innovation and entrepreneurship training program (No. S202210904026) and the Doctoral Research Initiation Fund of Zaozhuang University (Nos. 745010116, 1020727).

## Disclosure

The authors declare that they have no competing interests.

## References

1. Ding NH, Li JJ, Sun LQ. Molecular mechanisms and treatment of radiation-induced lung fibrosis. *Curr Drug Targets*. 2013;14(11):1347–1356. doi:10.2174/13894501113149990198
2. Postma DS, Timens W. Remodeling in asthma and chronic obstructive pulmonary disease. *Proc Am Thorac Soc*. 2006;3(5):434–439. doi:10.1513/pats.200601-006AW
3. Ramirez AM, Shen Z, Ritzenthaler JD, Roman J. Myofibroblast transdifferentiation in obliterative bronchiolitis: tgf-beta signaling through smad3-dependent and -independent pathways. *Am J Transplant*. 2006;6(9):2080–2088. doi:10.1111/j.1600-6143.2006.01430.x
4. Kong FM, Hayman JA, Griffith KA, et al. Final toxicity results of a radiation-dose escalation study in patients with non-small-cell lung cancer (NSCLC): predictors for radiation pneumonitis and fibrosis. *Int J Radiat Oncol Biol Phys*. 2006;65(4):1075–1086. doi:10.1016/j.ijrobp.2006.01.051
5. Shintani S, Mihara M, Li C, et al. Up-regulation of DNA-dependent protein kinase correlates with radiation resistance in oral squamous cell carcinoma. *Cancer Sci*. 2003;94(10):894–900. doi:10.1111/j.1349-7006.2003.tb01372.x
6. Chen AY, Zhang K, Liu GQ. LncRNA LINP1 promotes malignant progression of pancreatic cancer by adsorbing microRNA-491-3p. *Eur Rev Med Pharmacol Sci*. 2020;24(18):9315–9324. doi:10.26355/eurrev\_202009\_23013
7. Huang YA, Chan K, You ZH, Hu P, Wang L, Huang ZA. Predicting microRNA-disease associations from lncRNA-microRNA interactions via Multiview Multitask Learning. *Brief Bioinform*. 2021;22(3). doi:10.1093/bib/bbaa133
8. Paraskevopoulou MD, Hatzigeorgiou AG. Analyzing MiRNA-LncRNA interactions. *Methods Mol Biol*. 2016;1402:271–286. doi:10.1007/978-1-4939-3378-5\_21
9. Tay Y, Rinn J, Pandolfi PP. The multilayered complexity of ceRNA crosstalk and competition. *Nature*. 2014;505(7483):344–352. doi:10.1038/nature12986
10. Wu J, Huang H, Huang W, Wang L, Xia X, Fang X. Analysis of exosomal lncRNA, miRNA and mRNA expression profiles and ceRNA network construction in endometriosis. *Epigenomics*. 2020;12(14):1193–1213. doi:10.2217/epi-2020-0084
11. Zhang H, Bian C, Tu S, et al. Integrated analysis of lncRNA-miRNA-mRNA ceRNA network in human aortic dissection. *BMC Genomics*. 2021;22(1):724. doi:10.1186/s12864-021-08012-3
12. Kobayashi H, Tomari Y. RISC assembly: coordination between small RNAs and Argonaute proteins. *Biochim Biophys Acta*. 2016;1859(1):71–81. doi:10.1016/j.bbagr.2015.08.007
13. Arroyo-Hernandez M, Maldonado F, Lozano-Ruiz F, Munoz-Montano W, Nunez-Baez M, Arrieta O. Radiation-induced lung injury: current evidence. *BMC Pulm Med*. 2021;21(1):9. doi:10.1186/s12890-020-01376-4
14. Li Y, Zou L, Yang X, et al. Identification of lncRNA, microRNA, and mRNA-associated CeRNA network of radiation-induced lung injury in a mice model. *Dose-Response*. 2019;17(4):1559325819891012. doi:10.1177/1559325819891012
15. Xu P, Jia JQ, Jia JF, Jiang EJ. Radioprotective effects of troxerutin against gamma irradiation in V79 cells and mice. *Asian Pac J Cancer Prev*. 2011;12(10):2593–2596.
16. Xu P, Jia JQ, Jia JF, Jiang EJ. Radioprotective effects of troxerutin against gamma irradiation in mice liver. *Inter J Radiat Biol*. 2012;88(8):607–612. doi:10.3109/095553002.2012.692494
17. Xu P, Zhang WB, Cai XH, Qiu PY, Hao MH, Lu DD. Activating AKT to inhibit JNK by troxerutin antagonizes radiation-induced PTEN activation. *Eur J Pharmacol*. 2017;795:66–74. doi:10.1016/j.ejphar.2016.11.052
18. Yoon JH, Abdelmohsen K, Gorospe M. Functional interactions among microRNAs and long noncoding RNAs. *Semin Cell Dev Biol*. 2014;349–414. doi:10.1016/j.semcdb.2014.05.015
19. Luo Y, Zhang C, Tang F, et al. Bioinformatics identification of potentially involved microRNAs in Tibetan with gastric cancer based on microRNA profiling. *Cancer Cell Int*. 2015;15:115. doi:10.1186/s12935-015-0266-1
20. Zhang C, Zhu Y, Zhang Y, Gao L, Zhang N, Feng H. Therapeutic potential of umbilical cord mesenchymal stem cells for inhibiting myofibroblastic differentiation of irradiated human lung fibroblasts. *Tohoku J Exp Med*. 2015;236(3):209–217. doi:10.1620/tjem.236.209
21. Yang X, Shao J, Wu XM, et al. Troxerutin stimulates osteoblast differentiation of mesenchymal stem cell and facilitates bone fracture healing. *Front Pharmacol*. 2021;12:723145. doi:10.3389/fphar.2021.723145
22. Delbrel E, Soumare A, Naguez A, et al. HIF-1alpha triggers ER stress and CHOP-mediated apoptosis in alveolar epithelial cells, a key event in pulmonary fibrosis. *Sci Rep*. 2018;8(1):17939. doi:10.1038/s41598-018-36063-2
23. Pezzuto A, D'Ascanio M, Ricci A, Pagliuca A, Carico E. Expression and role of p16 and GLUT1 in malignant diseases and lung cancer: a review. *Thorac Cancer*. 2020;11(11):3060–3070. doi:10.1111/1759-7714.13651

### Publish your work in this journal

The Journal of Inflammation Research is an international, peer-reviewed open-access journal that welcomes laboratory and clinical findings on the molecular basis, cell biology and pharmacology of inflammation including original research, reviews, symposium reports, hypothesis formation and commentaries on: acute/chronic inflammation; mediators of inflammation; cellular processes; molecular mechanisms; pharmacology and novel anti-inflammatory drugs; clinical conditions involving inflammation. The manuscript management system is completely online and includes a very quick and fair peer-review system. Visit <http://www.dovepress.com/testimonials.php> to read real quotes from published authors.

Submit your manuscript here: <https://www.dovepress.com/journal-of-inflammation-research-journal>